Electronic Supplementary Material (ESI) for Nanoscale.

Supplemental Information
for
"Squeezed Nanocrystals: Equilibrium Configuration of Metal Clusters Embedded Beneath the Surface of a Layered Material"

Scott E. Julien,[1] Ann Lii-Rosales,[2,3] Kai-Tak Wan,[1] Yong Han,[2,4]
Michael C. Tringides,[2,4] James W. Evans,[2,4] and Patricia A. Thiel[2,3,5]

[1]Mechanical and Industrial Engineering, Northeastern University, Boston, MA 02115 USA
[2]Ames Laboratory, Ames, Iowa 50011 USA
[3]Department of Chemistry, Iowa State University, Ames, IA 50011 USA
[4]Department of Physics and Astronomy, Iowa State University, Ames, IA 50011 USA
[5]Department of Materials Science and Engineering, Iowa State University, Ames, IA 50011 USA

Contents.

1. Methods.

Determination of dimensions from STM data. The dimensions of Cu (and Fe) islands were measured from the experimental data by using an open-access software for STM image processing, WSxM.[1] Specifically, the annular width *a* was measured from derivative STM images where the image contrast is enhanced and the annulus has a clear boundary. The annular width is taken as the distance between edges of island top and bottom, as shown in Fig. SI-1 below. Island top width *d* was also measured from derivative STM images. Measurements in several different directions were taken and averaged to generate *d*, especially in consideration of islands that have a more non-isotropic shape, i.e., elongated hexagons. Island height *h* was obtained from pixel height histograms generated by the "roughness analysis" feature in WSxM. The above measurement procedures were carried out systematically island-by-island, for a total of 140 Cu islands and 140 Fe islands.

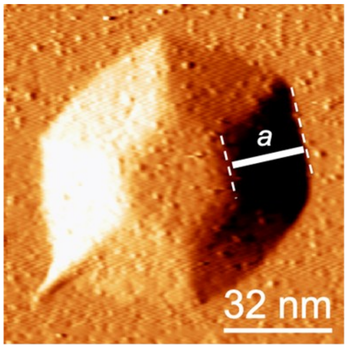

Figure SI-1. An encapsulated Cu island with annular width a labeled. Note the width is measured perpendicular to both edges contoured by dashed lines.

Mathematica. The commercial symbolic mathematical manipulation software, Mathematica©, was used to perform the algebraic operations, as well as the subsequent numerical computations used to generate the graphs.

DFT. Full details of our DFT results are given in Ref. 14 of the main text. Here we provide some basic information.

We performed first-principles DFT total-energy calculations for the Cu, graphite-graphene, Cu-graphite, and Cu-graphene systems using the Vienna Ab Initio Simulation Package (VASP) code.[2] The projector-augmented-wave (PAW) method[3] was used for the electron-core interactions. The pseudopotentials were generated and released in 2013 by the VASP group. For all Cu-C systems, as well as pure C, we used the optB88-vdW functional, where the exchange functional was optimized for the correlation part,[4] to approximately account for dispersion interactions. For pure Cu we used PBEsol GGA.[5] These choices of functionals were made after comparing results from various functionals, and benchmarking the results against experimental data. Spin-polarization effects and dipole corrections were taken into account in all DFT calculations. The Γ-centered $\boldsymbol{k}$ mesh varied with the system. The vacuum thickness between two adjacent slab replicas was not less than 1.6 nm. The force-convergence criterion was 0.1 eV/nm.

Values of surface energies and adhesion energies, in Table 1 of the main text, were derived from models that incorporated multiple layers of graphene and copper. For instance, the graphite substrate was represented by at least 6 layers of graphene for calculation of graphite-graphene adhesion energy β_{GnGt}, and copper-graphite adhesion energy β_{CuGt}. Calculations were tested carefully to ensure that a sufficient number of layers was used in every case.

2. Formulation of the Energy Associated with a Generic Intercalated Metal Cluster

A convenient and systematic way to obtain an appropriate expression for the total energy, Π, associated with an adsorbed or intercalated cluster is to start by considering the energy of an unsupported cluster, and then to account for energy changes upon adsorption and intercalation. Here, we take the shape of the unsupported cluster to match that of the final adsorbed or intercalated cluster. Below, contributions to the total energy will be labeled as $U_\alpha > 0$, for various α. For the unsupported (unsupp) cluster of metal M, we write $\Pi_{unsupp} = -U_{bulk} + U_M$. Here, the bulk energy has the form $U_{bulk} = N\,E_{bulk}$ where N is the number of M atoms and E_{bulk} is the energy per atom for bulk M cohesive energy. The surface energy cost has the form, $U_M = \sum_j \gamma_M{}^j A_j$, where $\gamma_M{}^j$ is the surface energy (per unit area) associated with facet j, and A_j is the corresponding surface area.

For an adsorbed or supported (supp) M cluster on an extended substrate labeled X, Π_{supp} is lowered relative to the unsupported case by adhesion to the substrate. Thus, we write

$$\Pi_{supp} = \Pi_{unsupp} - U_{MX},$$

where $U_{MX} = \beta_{MX}\,A_{base}$, with β_{MX} denoting the adhesion energy (per unit area) of M to the substrate, X, and A_{base} the area of the base facet of the cluster in contact with the substrate X.

For an intercalated (interc) M cluster, the substrate X is a layered material (e.g., graphite) and during intercalation is partitioned as $X = X\text{-} + X\text{+}$ where X- corresponds to the portion of the substrate underneath the M cluster (e.g., an infinite number of graphene layers) and X+ is the portion covering the M cluster (e.g., a few graphene layers). Now Π_{interc} is lowered relative to the unsupported case by adhesion both to the underlying support, X-, and to the covering portion, X+. However, there is also an energy cost associated with delaminating a portion of the underlying support from the covering portion and with the strain energy induced by intercalation which we argue is mainly confined to the strongly distorted covering layers X+. Thus, we write

$$\Pi_{interc} = \Pi_{unsupp} - U_{MX-} - U_{MX+} + U_{X-\,X+} + U_e.$$

Here, one has $U_{MX-} = \beta_{MX-}\,A_{base}$ and $U_{MX+} = \beta_{MX+}\,A_{top}$ with β_{MX-} (β_{MX+}) denoting the adhesion energy (per unit area) of M to X- (X+), and A_{base} (A_{top}) the area of the base (top) facet of the cluster in contact with X- (X+). Also, one has that $U_{X-\,X+} = \beta_{X-\,X+}\,A_{delam}$ with $\beta_{X-\,X+}$ denoting the adhesion energy (per unit area) of X- to X+, and A_{delam} denoting the area over which X- and X+ are separated. Finally, U_e denotes the total strain energy cost (taken as mainly confined to X+).

Since our focus is on the equilibrium structure of intercalated M clusters for fixed M cluster size, the term U_{bulk} is fixed so we drop this term and minimize

$$\Pi_{interc} = U_M + U_{X-\,X+} - U_{MX-} - U_{MX+} + U_e.$$

3. Expressions for Elastic Stretching and Bending Energies in the Clamped SLBT Model.

$$U_{e,s,cl} = \frac{Yt \qquad \pi^2 \qquad 1}{(1-\nu^2)\frac{\pi}{4}\left[(d+2a)^2-d^2\right]Log\left[\left(\frac{d}{d+2a}\right)^2\right]^2}h^4$$

Eq. SI-1

$$U_{e,b,cl} = \frac{8}{3}\frac{\pi Y t^3}{(1-\nu^2)}\frac{(d+2a)^2 - d^2}{\left[(d+2a)^2 - d^2\right]^2 - (d+2a)^2 d^2 Log\left[\left(\frac{d}{d+2a}\right)^2\right]^2} h^2 \quad \text{Eq. SI-2}$$

4. Comprehensive Key to Subscripts Used in the Equations.

CuGn	copper-graphene
CuGt	copper-graphite
CuG	copper-graphite and copper-graphene
GnGt	graphene-graphite
CuTp	top of copper cluster
CuSd	side of copper cluster
e	elastic strain
s	stretching
b	bending
fr	free SLBT model
cl	clamped SLBT model

5. Supplemental Figures.

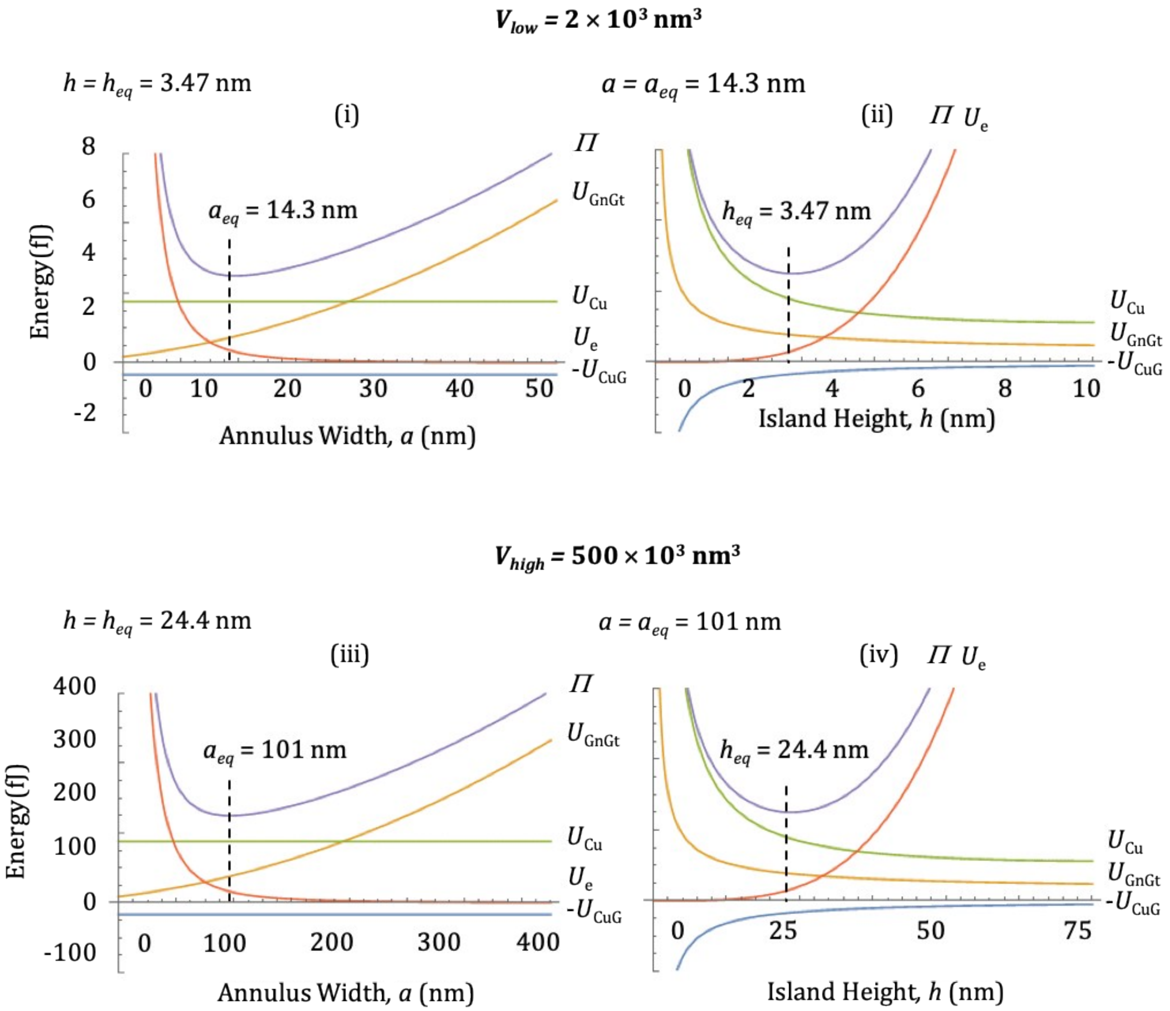

Figure SI-2. Energy vs. *h* or *a* for islands with different total fixed volume and $L = 4$, using the free SLBT model. Panels (i, ii) represent an island volume at the low end of the range of observations, $V_{low} = 2 \times 10^3$ nm^3. Panels (iii, iv) represent an island volume at the high end of the observed range, $V_{high} = 5 \times 10^5$ nm^3. Qualitatively, these graphs are very similar to Fig. 2(c,d) where the volume is intermediate, 4×10^4 nm^3. These data illustrate that the qualitative energetic balance governing equilibrium island dimensions, in the SLBT model, does not change over a range that spans over 2 orders of magnitude in *V*. The balance also depends only weakly on whether the SLBT model is free or clamped (not shown).

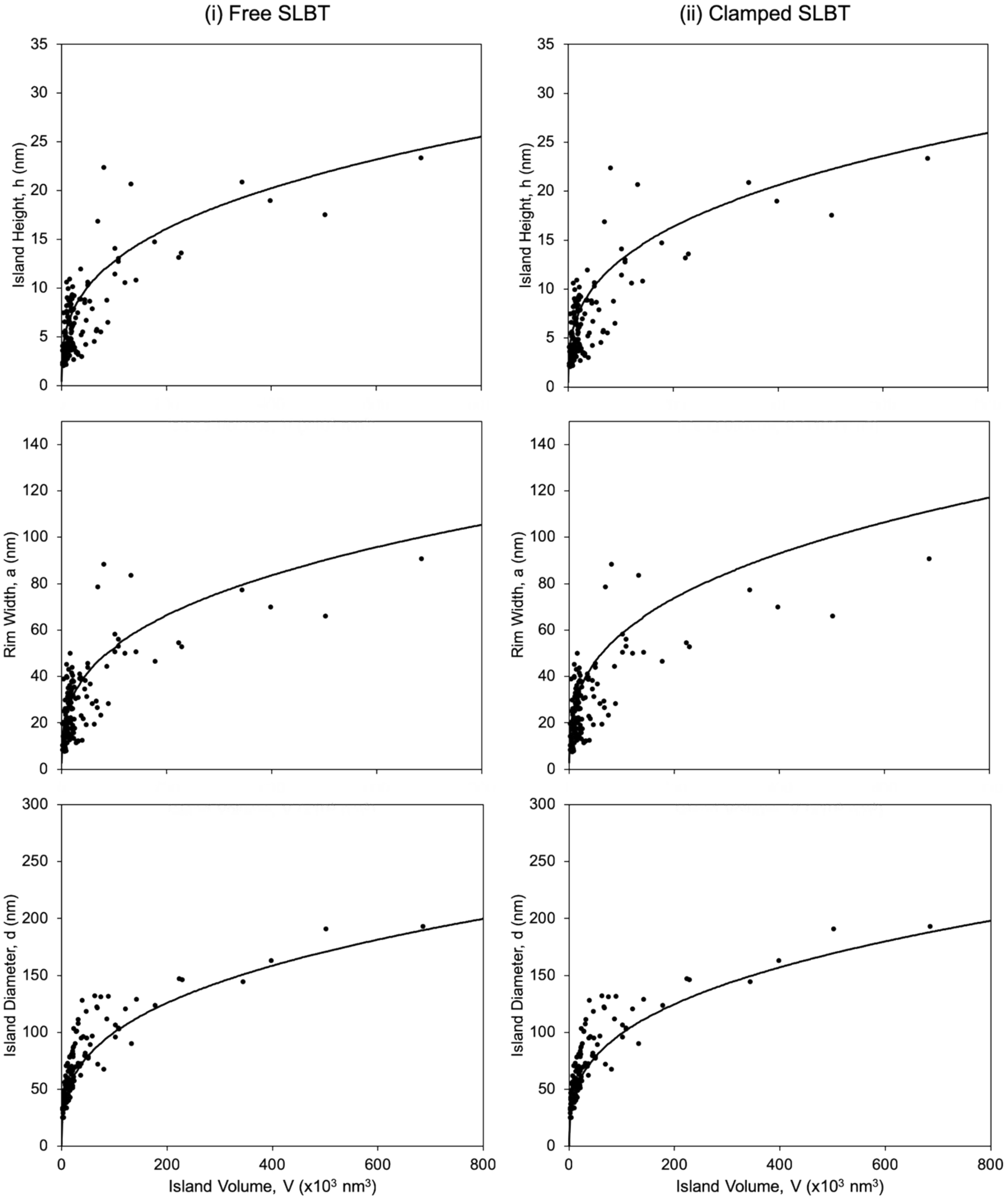

Figure SI-3. Island dimensions *h, a*, and *d* as functions of *V* for *L* = 4, in the (i) free and (ii) clamped SLBT model.

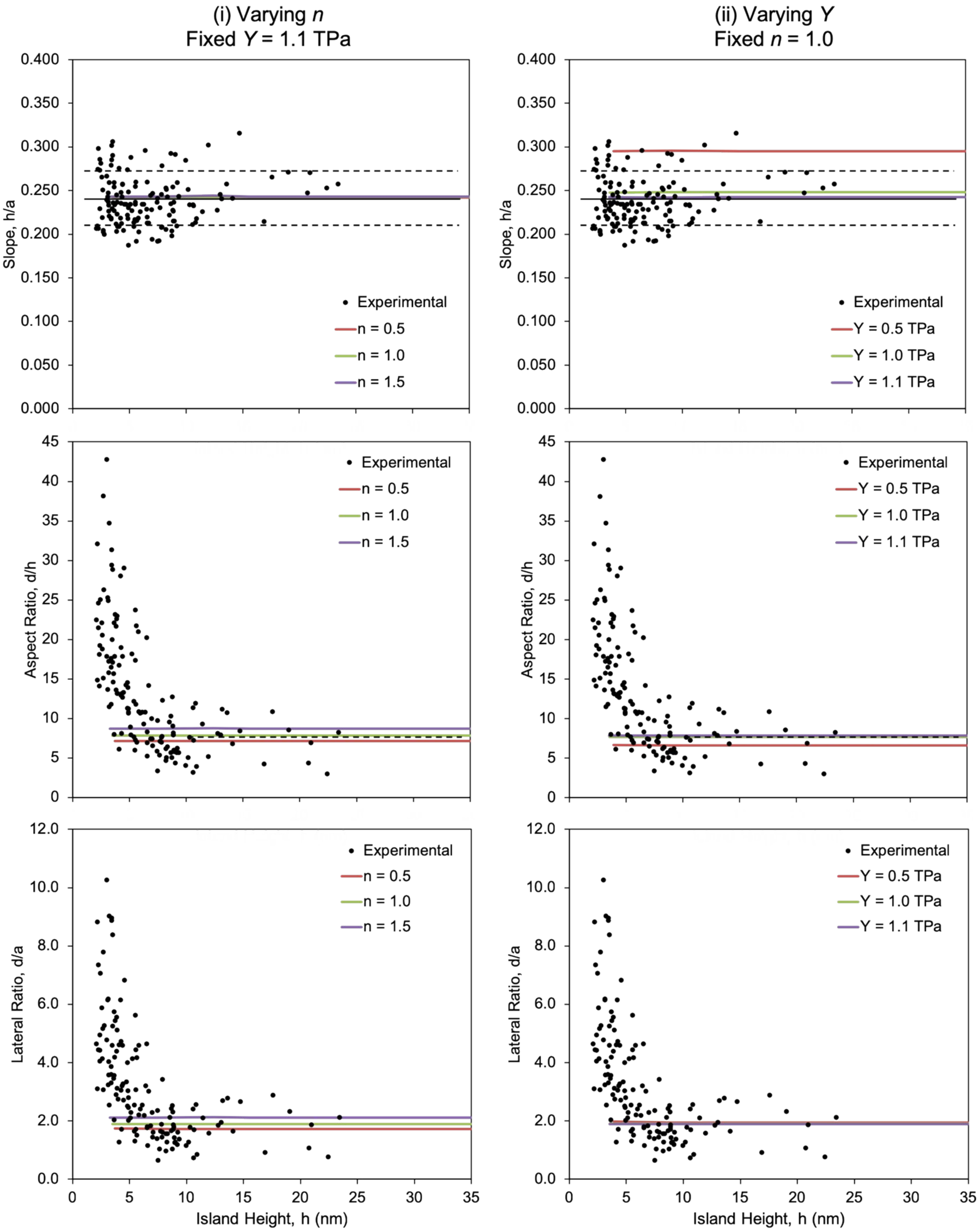

Figure SI-4. Sensitivity analyses for the free SLBT model with *L*=4. (a) Dependence on the U_{CuG} term. Here *n* is a factor applied to U_{CuG}. (b) Dependence on Young's modulus, *Y*. The optimal value is regarded to be *Y* = 1.1 TPa.

In Fig. SI-4, the two parameters U_{CuG} and Y are chosen for sensitivity analysis because we regard them as having highest uncertainty.

The uncertainty in U_{CuG} arises from uncertainty in the adhesion energy, β_{CuG}, between Cu(111) and graphite or graphene. This value is calculated from density functional theory (DFT).[6] In the DFT calculations, a Cu slab is compressed by 3.9% from its bulk lattice constant to obtain registry with the graphite/graphene, thereby creating a supercell that is computationally-tractable. The effect of this strain on the adhesion energy is unclear. In experimental data, moiré patterns are often reported for graphene on Cu(111), which suggests that the real supercell is larger than that used for DFT, at least for the Cu-graphene interface.[7-9] However, as discussed in the main text, the U_{CuG} energy term contributes little to determining the minimum in total energy $\Pi(a,h)$. Hence the results of the model are not significantly sensitive to n.

The Young's modulus of graphene, Y, is directly proportional to the energy term U_e as shown in Eq. 4 of the main text or Eq. SI1 above. The uncertainty in Y arises from the variety of results reported in the literature, ranging from 0.2 to 1.1 TPa for graphene. As noted in the main text, our preferred value is 1.1 TPa because that value has been measured under conditions that most closely correspond to our experiment, including defect density. The sensitivity analysis shows that reducing this to 1.0 TPa, which is a value reported for pristine graphene in several papers,[10-13] has negligible effect. A reduction to 0.5 TPa has a significant effect on h/a but not on d/h or d/a.

6. References for Supplemental Information.

1. Horcas, I.; Fernández, R.; Gómez-Rodríguez, J. M.; Colchero, J.; Gómez-Herrero, J.; Baro, A. M., WSXM: A software for scanning probe microscopy and a tool for nanotechnology. *Rev. Sci. Instrum.* **2007,** *78* (1), 013705.
2. G. Kresse, J. F., Efficient iterative schemes for ab initio total-energy calculations using a plane-wave basis set. *Phys. Rev. B* **1996,** *54*, 11169-11186.
3. Kresse, G.; Joubert, D., From ultrasoft pseudopotentials to the projector augmented-wave method. *Phys. Rev. B* **1999,** *59* (3), 1758-1775.
4. Jiří, K.; David, R. B.; Angelos, M., Chemical accuracy for the van der Waals density functional. *J. Phys.: Condens. Matter* **2010,** *22* (2), 022201.
5. Perdew, J. P.; Ruzsinszky, A.; Csonka, G. I.; Vydrov, O. A.; Scuseria, G. E.; Constantin, L. A.; Zhou, X.; Burke, K., Restoring the Density-Gradient Expansion for Exchange in Solids and Surfaces. *Phys. Rev. Lett.* **2008,** *100* (13), 136406.
6. Han, Y.; Lai, K. C.; Lii-Rosales, A.; Tringides, M. C.; Evans, J. W.; Thiel, P. A., Surface energies, adhesion energies, and exfoliation energies relevant to copper-graphene and copper-graphite systems. *Submitted* **2018**.
7. Gao, L.; Guest, J. R.; Guisinger, N. P., Epitaxial graphene on Cu(111). *Nano Lett.* **2010,** *10* (9), 3512-3516.
8. Süle, P.; Szendrő, M.; Hwang, C.; Tapasztó, L., Rotation misorientated graphene moiré superlattices on Cu (111): Classical molecular dynamics simulations and scanning tunneling microscopy studies. *Carbon* **2014,** *77*, 1082-1089.

9. Gottardi, S.; Müller, K.; Bignardi, L.; Moreno-López, J. C.; Pham, T. A.; Ivashenko, O.; Yablonskikh, M.; Barinov, A.; Björk, J.; Rudolf, P.; Stöhr, M., Comparing Graphene Growth on Cu(111) versus Oxidized Cu(111). *Nano Lett.* **2015,** *15* (2), 917-922.
10. Lee, C.; Wei, X.; Kysar, J. W.; Hone, J., Measurement of the Elastic Properties and Intrinsic Strength of Monolayer Graphene. *Science* **2008,** *321* (5887), 385-388.
11. Changgu, L.; Xiaoding, W.; Qunyang, L.; Robert, C.; W., K. J.; James, H., Elastic and frictional properties of graphene. *Phys. Status Solidi B* **2009,** *246* (11 ‐ 12), 2562-2567.
12. Koenig, S. P.; Boddeti, N. G.; Dunn, M. L.; Bunch, J. S., Ultrastrong adhesion of graphene membranes. *Nat. Nanotechnol.* **2011,** *6*, 543.
13. Huang, M.; Pascal, T. A.; Kim, H.; Goddard, W. A.; Greer, J. R., Electronic−Mechanical Coupling in Graphene from in situ Nanoindentation Experiments and Multiscale Atomistic Simulations. *Nano Lett.* **2011,** *11* (3), 1241-1246.